MIRAE Vol. 2, No. 2, December 2025
ISSN: 3063-8720, DOI: 10.70935/y4n8aq82

Article

Comparative Mechanical Performance of FDM-Printed PETG and ABS at Different Infill Percentages

Saeful Rofi Romadhon[1,2,*], Baharudin Priwintoko[1,3], Wahyu Hidayat[1], Baskara Surya Widagdo[1]

[1]Department of Mechanical Engineering, Universitas Diponegoro, Semarang, Indonesia
[2]Department of Mechanical Engineering, Faculty of Science, Technology, and Health, Muhammadiyah University of Brebes, Jl. Pangeran Diponegoro No. 184, Grengseng, Paguyangan, 52276, Indonesia
[3]Department of Mechanical Engineering, Akademi Inovasi Indonesia, Salatiga, Indonesia
* Corresponding: rofiramadhann99@gmail.com

ARTICLE INFO

Submitted 7 Nov 2025
Revised 20 Dec 2025
Accepted 21 Dec 2025
Published 31 Dec 2025

Abstract

The use of Fused Deposition Modeling (FDM) in additive manufacturing requires a material selection strategy that considers not only strength, but also the balance between stiffness, ductility, toughness, and surface resistance. This study evaluates the comparative mechanical performance of Acrylonitrile Butadiene Styrene (ABS) and Polyethylene Terephthalate Glycol (PETG) at 25%, 50%, 75%, and 100% infill using FDM printing and performance-map analysis. Specimens were designed according to ASTM standards and printed using the same printer, hexagonal infill pattern, print speed, and build orientation, while material-specific parameters such as extrusion temperature, heated bed temperature, layer height, first-layer height, enclosure, and cooling fan setting were adjusted according to ABS and PETG processing requirements. Mechanical characterization included tensile, flexural, impact, Shore D hardness, and density tests. The highest tensile strength was obtained by PETG at 100% infill, reaching 40.74 MPa, while ABS at the same infill reached 38.72 MPa. PETG also showed the highest elongation at break of 16.16%, flexural strength of 59.51 MPa, and impact strength of 0.053 J/mm². In contrast, ABS produced the highest surface hardness, reaching 84.17 Shore D at 100% infill, compared with 80.42 Shore D for PETG. The density values of both materials increased with infill and became similar at 100% infill, namely 1.00 g/cm³. These findings confirm a clear trade-off between strength, toughness, resilience, and hardness in FDM materials. PETG offers a more balanced mechanical profile for applications that require strength, deformation tolerance, and impact resistance, while ABS remains relevant for applications that prioritize rigidity and surface hardness.

Keywords: Fused Deposition Modeling; ABS; PETG; Infill density; Mechanical performance mapping

ISSN: 3063-8720, DOI: 10.70935/y4n8aq82

INTRODUCTION

Studies on fused deposition modeling (FDM) as an additive manufacturing (AM) technology in the industrial sector have increased significantly. This is driven by its ability to produce high design freedom, efficient use of materials, and relatively competitive process costs [1], [2], [3]. FDM is one of the most widely used AM methods, working by extruding thermoplastic material through a heated nozzle and forming objects gradually layer by layer according to a predetermined print path [4], [5], [6].

Acrylonitrile Butadiene Styrene (ABS) is a material commonly used in the FDM process due to its toughness, impact resistance, and relative stability under dynamic loads [7], [8]. However, ABS has several limitations, such as a tendency to warp, the need for high printing temperatures, and particle and vapor emissions during the printing process, which may limit its use in certain applications [9], [10], [11]. Therefore, the development and utilization of alternative materials are important for expanding the applications of FDM.

In 2025, Romadhon et al conducted a comparative study between Polylactic Acid (PLA) and ABS fabricated using the FDM method with identical printing parameters and testing standards. The results of this study showed significant differences in mechanical characteristics between the two materials, confirming the importance of selecting the right material according to application requirements [2].

Polyethylene Terephthalate Glycol (PETG) has emerged as a widely used material in FDM-based 3D printing due to its combination of mechanical strength, flexibility, chemical resistance, and ease of processing [12], [13], [14]. PETG is between PLA and ABS, with better impact resistance and flexibility than PLA, as well as being more stable against distortion and producing lower emissions than ABS [15], [14], [16]. In addition, PETG's transparency and biocompatibility expand its potential for medical and biomedical applications [12], [17], [18]. However, comprehensive understanding of the mechanical performance of PETG relative to ABS, particularly when fabricated using identical printing parameters, remains limited.

Several studies have examined the mechanical performance of FDM-fabricated ABS and PETG through optimization of internal structure parameters. Yah Yun Aw et al. [19] shows that increasing the infill density in ABS significantly increases tensile strength and flexural strength due to reduced porosity and improved interlayer bonding. Mahandika and Sukma [20] reported that variations in infill density (25–100%) in ABS+ significantly increased tensile strength starting at a density of 75%, with a maximum value of 17.10 N/mm² at 100% infill. In PETG material, Srinivasan et al. [21] found that an increase in infill density is directly proportional to tensile strength, with the highest value being around 32.12 MPa at 100% infill. Hozdić and Hozdić [22]

shows that the shape and density of the infill significantly affect the maximum force and breaking force on PETG and carbon fiber reinforced PETG (PETG+CF). In addition, Kumaresan and Kanny [23] reported a maximum tensile strength of 43.09 MPa on PETG through optimization of the infill pattern and raster angle using Response Surface Methodology (RSM), with the raster angle as the most influential parameter.

Most previous studies have focused on PLA materials or analyzed the effects of process parameters partially, such as variations in infill density, print orientation, and layer thickness [24], [25]. The novelty of the present work lies in its direct PETG-ABS comparison across five property groups, namely tensile strength, elongation at break, flexural strength, impact strength, hardness, and density, using the same printer platform, ASTM-based specimen geometry, hexagonal infill architecture, and the same infill levels. Instead of discussing a single mechanical property, this study integrates the results into material performance maps so that the strength-ductility, flexural-impact, and hardness-density trade-offs can be interpreted simultaneously. This approach provides a more practical basis for selecting FDM materials according to the required balance between stiffness, toughness, ductility, and surface resistance.

METHODS

Materials and Specimens

The materials used in this study were ABS and PETG filaments with a diameter of 1.75 mm. The specimens were designed using SolidWorks software with reference to the relevant ASTM testing standards. The three-dimensional model was then converted into STL format and process

ed using FlashPrint software to determine the printing parameters and slice it into print layers. The fabrication stage was carried out using a Flashforge Dreamer 3D printer based on the Fused Deposition Modeling (FDM) method. Details of the technical specifications of the equipment used are presented in Table 1.

Table 1. Flashforge Dreamer printer specifications [2]

	Flashforge Dreamer
Printing Technology	FFF (Fused Filament Fabrication)
Printer Dimensions	480 x 335 x 410 mm
Print Dimensions	230 L x 150 W x 140 H
Layer Resolution	100 - 500 microns
Position Precision	XY : 11 microns, Z : 2,5 microns
Software and Firmware	FlashPrint
Number of Extruders	2
Connectivity	Wi-Fi, USB Cable, SD Card
Heated Bed	*Yes*
AC input	100-240 V, ~2amps. 50-60Hz, 350W

ISSN: 3063-8720, DOI: 10.70935/y4n8aq82

The printing process was designed to keep the comparison as controlled as possible while still using material-appropriate printing conditions. Nozzle diameter, infill pattern, infill percentage, print speed, travel speed, wall configuration, and build orientation were kept constant for ABS and PETG. However, nozzle temperature, bed temperature, layer height, first-layer height, enclosure condition, and cooling fan setting were adjusted according to the processing requirements of each material to reduce warping, improve first-layer adhesion, and avoid poor interlayer bonding. Therefore, the comparison should be interpreted as a practical comparison between optimized ABS and optimized PETG printing conditions rather than a comparison in which only one process parameter was varied.

The main variation in this study was the infill percentage of 25%, 50%, 75%, and 100% with a hexagonal pattern, which was chosen because it provides a more even stress distribution. Other parameters such as wall thickness and print orientation were kept constant, so that the research variables focused on the type of material (ABS and PETG) and infill variations. Details of the configuration are presented in Table 2.

Table 2. Printing parameter configuration

Settings	Material	
	ABS	**PETG**
Nozzle Temperature (°C)	240	235
Bed Temperature (°C)	110	80
Layer Height (mm)	0,18	0,2
First Layer Height (mm)	0,27	0,3
Infill Shape	Hexagon	Hexagon
Infill Percentage (%)	25, 50, 75, 100	25, 50, 75, 100
Print Speed (mm/s)	60	60
Travel Speed (mm/s)	80	80
Enclosure	yes	no
Fan	Nozzle Only	All On

In this study, five replicates of test specimens were made for each test condition. Thus, a total of 40 specimens were obtained for each type of mechanical test, consisting of two types of materials, four variations in infill density, and five replicates. Tensile test specimens were produced based on ASTM D638 Type I, while bending tests referred to ASTM D790. Impact testing was carried out in accordance with ASTM D256, and surface hardness measurements were determined using the Shore D method based on ASTM D2240. Meanwhile, density testing was carried out with reference to ASTM D792. The dimensions of the test specimens for each test are presented in detail in Figures 1 to 5 in millimeters.

ISSN: 3063-8720, DOI: 10.70935/y4n8aq82

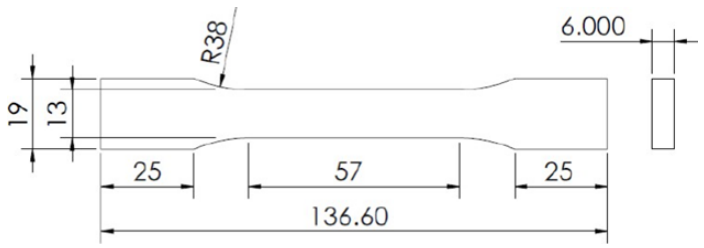

Figure 1. Dimensions of tensile test specimens [2]

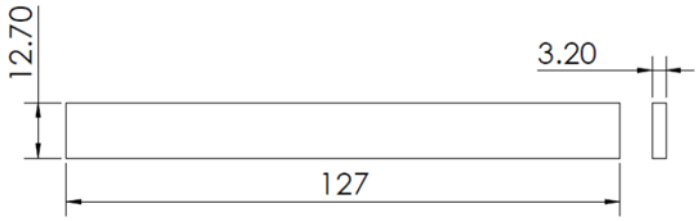

Figure 2. Dimensions of the bending test specimen [2]

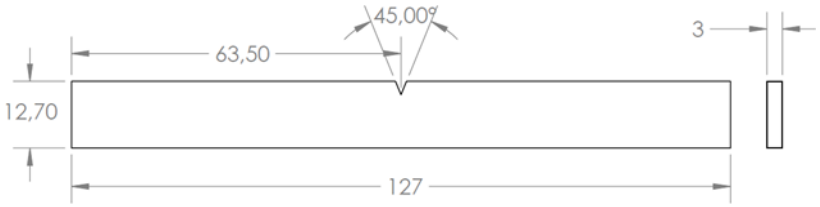

Figure 3. Impact test specimen dimensions [2]

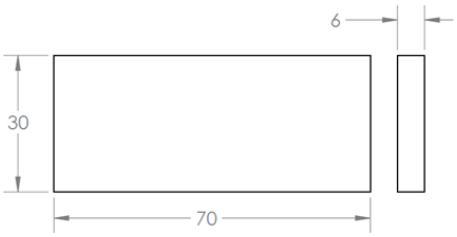

Figure 4. Dimensions of hardness test specimens [2]

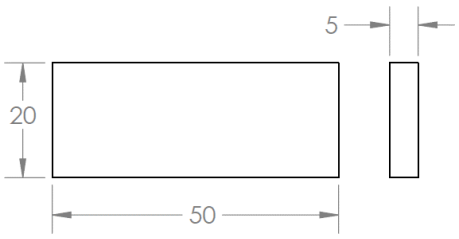

Figure 5. Dimensions of density test specimens [2]

ISSN: 3063-8720, DOI: 10.70935/y4n8aq82

Mechanical Testing Procedures

Mechanical testing was conducted based on ASTM standards to obtain comprehensive material characterization. Tensile testing was performed using a 50 kN UTM with a crosshead speed of 5 mm/minute in accordance with ASTM D638 to determine UTS, elongation at break, and elastic modulus. Flexural testing used the three-point bending method in accordance with ASTM D790 with a span distance of 16 times the thickness of the specimen to obtain the flexural strength and modulus. Impact testing was performed using a 2 J pendulum impact tester in accordance with ASTM D256 to determine the toughness of the material. Surface hardness is measured using a Shore D durometer based on ASTM D2240 with three test points per specimen. Material density is determined based on ASTM D792 using Archimedes' principle. All testing equipment is calibrated before testing to ensure the accuracy of the results.

Data Analysis

The tensile, flexural, impact, hardness, and density test data were quantitatively analyzed for each material-infill combination. The reported values represent the mean of five specimens for each condition (n = 5), which reduces the influence of specimen-to-specimen variation in the FDM process. Because the available manuscript dataset contains only the averaged values and does not include the individual replicate readings, standard deviation, coefficient of variation, and inferential significance testing could not be recalculated for the present revision. Accordingly, the comparison is treated as descriptive and trend-based. Future work should report the raw replicate data together with standard deviation, confidence intervals, and analysis of variance to strengthen statistical reliability.

To evaluate the overall correlation between mechanical properties, the data was mapped in the form of scatter plot-based material performance maps. The performance maps used included: (i) the relationship between maximum tensile stress and fracture strain, (ii) the relationship between bending stress and impact energy, and (iii) the relationship between hardness and density. Each point on the map represents a unique material–infill combination, so that the systematic shift in point position reflects the influence of internal architecture variations on the mechanical response of the material.

This mapping approach allows the identification of trade-offs between mechanical properties, such as between increased strength and decreased ductility, without simplifying the data into a single performance index. Thus, the mechanical characteristics of materials can be analyzed multidimensionally in accordance with the principle of performance-based material selection. The comparison between ABS and PETG is based on relative position, distribution trends, and the trajectory of mechanical property changes on each performance

ISSN: 3063-8720, DOI: 10.70935/y4n8aq82

map, allowing for a comprehensive evaluation of material response differences to infill variations.

RESULT AND DISCUSSION

Tensile Test, Bending Test, Impact Test, Hardness Test, and Density Test

The values in Table 3 are mean values from five specimens per condition (n = 5). The individual replicate values were not available in the manuscript dataset; therefore, dispersion statistics are acknowledged as a limitation rather than estimated artificially.

Table 3. Summary of mean ABS and PETG mechanical testing results (n = 5)

Infill	Tensile Strength (MPa)		Elongation at Break (%)		Flexural Strength (MPa)		Impact Strength (J/mm²)		Hardness (Shore D)		Density (g/cm³)	
	ABS	PETG	ABS	PETG	ABS	PETG	ABS	PETG	ABS	PETG	ABS	PETG
25%	12.90	14.98	10.79	12.73	34.87	41.37	0.019	0.019	60.67	56.92	0.54	0.54
50%	16.06	18.80	10.73	15.78	41.93	43.90	0.038	0.037	77.83	70.33	0.72	0.70
75%	19.51	23.63	10.19	13.42	51.68	55.10	0.038	0.054	82.92	78.92	0.83	0.81
100%	38.72	40.74	11.74	16.16	58.06	59.51	0.052	0.053	84.17	80.42	1.00	1.00

The test results table maps the mechanical characteristics of ABS and PETG at infill variations of 25-100%, including tensile strength, elongation at break, flexural strength, impact strength, hardness, and density. In general, increasing the infill strengthens the internal structure of the specimens and improves almost all mechanical parameters in both materials. This confirms that infill acts as a microarchitecture that controls stress distribution paths, load-bearing cross-sectional area, void fraction, and failure mechanisms in FDM products.

PETG consistently demonstrates superior mechanical performance in terms of tensile and flexural strength, accompanied by higher elongation compared to ABS. This combination places PETG in the "strong-ductile" material domain, while ABS tends to be "strong-rigid." In impact tests, the difference between the two materials becomes more apparent at medium to high infill, where PETG shows better energy absorption capabilities. Conversely, ABS maintains higher surface hardness values, although the difference becomes smaller at high infill.

The density values of both materials increase with increasing infill and show very little difference at equivalent infill levels. This similarity is primarily attributed to the identical specimen geometry and the same nominal infill percentages used in slicing, which caused the bulk printed density to be governed more by the programmed solid fraction and void volume than by the

ISSN: 3063-8720, DOI: 10.70935/y4n8aq82

small difference in intrinsic filament density. Because density was determined as bulk specimen density, it includes the contribution of internal pores and printed architecture. Therefore, similar density values should not be interpreted as identical material composition, but as comparable printed solid fraction under the selected infill settings.

The Effect of Infill Percentage on the Tensile Behavior of ABS and PETG Materials

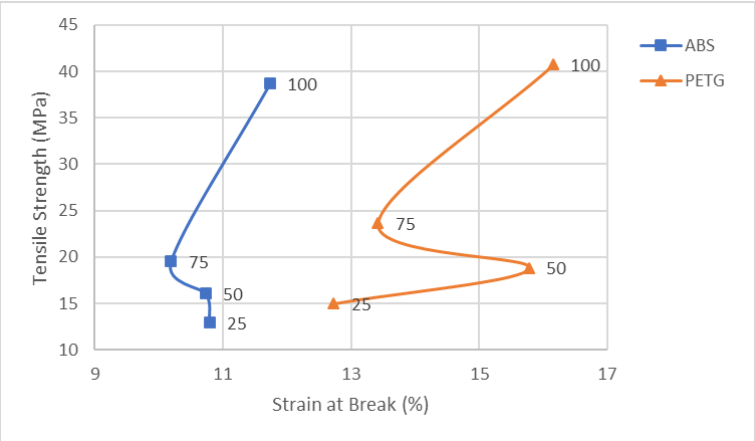

Figure 6. ABS and PETG stress-strain performance map at various infill levels

Figure 6 shows the relationship between infill percentage, maximum tensile stress, and fracture strain in ABS and PETG specimens produced using the Fused Deposition Modeling (FDM) process. The test results show that infill percentage is a key parameter that significantly affects tensile mechanical response, with different behavior characteristics in each material.

In ABS material, increasing the infill percentage from 25% to 100% resulted in a significant increase in tensile stress, from 12.9 MPa to 38.72 MPa. This increase is related to the reduction in internal porosity and the increase in effective cross-sectional area capable of transferring tensile loads. Conversely, the ABS fracture strain value is relatively stable in the range of 10–11%, even showing a slight downward trend at medium infill (50–75%). This indicates that the increase in internal density in ABS contributes more to strength improvement than to toughness improvement, making the material stiffer and more prone to brittle fracture at high infill.

Unlike ABS, PETG material shows a simultaneous increase in strength and toughness as the infill percentage increases. The tensile strength of PETG increases from 14.98 MPa at 25% infill to 40.74 MPa at 100% infill, accompanied by an increase in elongation at break from 12.73% to 16.16%. This behavior can be associated with better interlayer bonding, higher deformation tolerance, and the viscoelastic character of PETG. Under tensile loading, PETG can redistribute strain more gradually across deposited roads and layer

ISSN: 3063-8720, DOI: 10.70935/y4n8aq82

interfaces, delaying crack initiation and delamination. In contrast, ABS tends to show a more rigid response, so stress concentration at raster boundaries can promote earlier localized fracture.

Comparative analysis shows that across all infill variations, PETG has higher elongation at break than ABS, while the tensile strength values of both materials are relatively comparable at 100% infill. Thus, PETG is more suitable for applications that require resistance to deformation and energy absorption, while ABS is more appropriate for components that prioritize structural strength and rigidity.

Overall, these results confirm that infill percentage optimization must consider the interaction between the strength and toughness of the material, as well as the intrinsic mechanical characteristics of the filament used, in order to achieve optimal mechanical performance according to application requirements.

The Effect of Infill Percentage on the Flexural Strength and Impact Resistance of ABS and PETG Materials

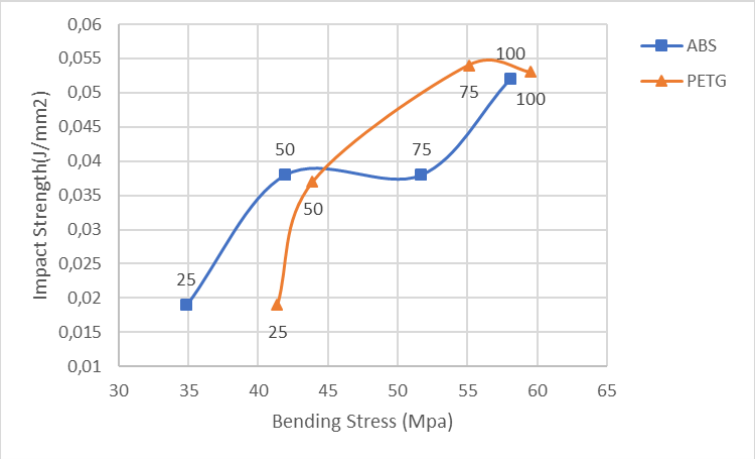

Figure 7. Flexural stress–impact strength performance map of ABS and PETG at various infill levels

The results of flexural and impact testing on ABS and PETG materials produced by Fused Deposition Modeling (FDM) show that the infill percentage plays a dominant role in determining flexural load-bearing capacity and energy absorption capability. An increase in infill generally increases flexural stress and impact strength due to reduced internal porosity and increased effectiveness of interlayer load transfer.

In ABS, flexural stress increased significantly from 34.87 MPa (25%) to 58.06 MPa (100%), along with increased structural stiffness. However, the increase in impact strength was not linear, with relatively stagnant values at 50–75% infill (≈0.038 J/mm²). This phenomenon indicates that even though the structure becomes stiffer, the failure mechanism of ABS is still dominated by

ISSN: 3063-8720, DOI: 10.70935/y4n8aq82

brittle crack propagation at the raster interface, so that the increase in density is not fully converted into impact toughness.

Conversely, PETG showed a simultaneous increase in flexural strength and impact toughness. Flexural strength increased from 41.37 MPa to 59.51 MPa, while impact strength rose from 0.019 J/mm² to 0.053 J/mm² with increasing infill. This response reflects more homogeneous interlayer bonding and viscoelastic deformation, which allow PETG to absorb impact energy through plastic deformation, strand stretching, and crack deflection before final failure. ABS, although stiffer, is more likely to localize damage at bead interfaces; therefore, the increase in infill does not translate as effectively into impact resistance.

A direct comparison shows that at high infill, PETG has a more balanced flexural strength to impact toughness ratio than ABS. Although the maximum flexural stress values of both materials are relatively comparable, PETG exhibits better crack and delamination resistance, making it more suitable for applications with dynamic flexural loads and shock loads.

Overall, these results confirm that infill optimization in FDM structures must consider the balance between stiffness and toughness, as well as the intrinsic mechanical characteristics of the material, in order to achieve optimal structural performance.

The Effect of Infill Percentage on the Hardness and Density of ABS and PETG Materials

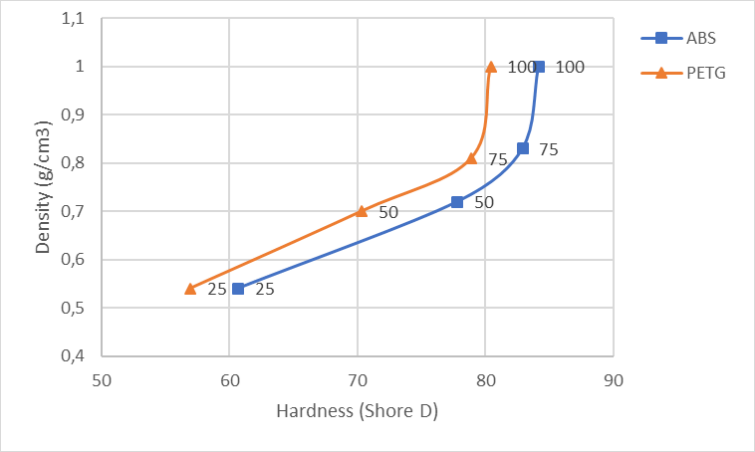

Figure 8. Hardness-density performance map of ABS and PETG at various infill levels

Increasing the infill percentage consistently increases the density and Shore D hardness of FDM-printed ABS and PETG, indicating a reduction in void fraction and an increase in solid material continuity. The density of both materials increases almost linearly from approximately 0.54 g/cm³ at 25% infill

ISSN: 3063-8720, DOI: 10.70935/y4n8aq82

to 1.00 g/cm³ at 100% infill, reflecting the effectiveness of infill percentage in controlling the internal structure.

In ABS, the increase in density was followed by a significant increase in hardness, from 60.67 Shore D to 84.17 Shore D, indicating the formation of a stiffer structure that is resistant to local deformation. In contrast, PETG exhibits lower hardness values at equivalent densities (56.92–80.42 Shore D), reflecting the viscoelastic character and intrinsic toughness of the material.

The difference in hardness response at comparable densities confirms that hardness is not solely controlled by density, but also by the intrinsic mechanical properties of the material and the quality of the interlayer bonds. Therefore, the selection of infill and material must consider the balance between surface rigidity and structural toughness requirements in FDM applications.

Discussion (Implications)

The results show that increasing infill percentage consistently increases specimen density, which directly contributes to higher tensile strength, flexural strength, impact toughness, and surface hardness in ABS and PETG materials produced by FDM. From a practical perspective, 100% infill gives the highest mechanical performance, but it also increases material use and printing time. Therefore, the infill level should be selected according to service requirements rather than maximized automatically. PETG is recommended for components subjected to dynamic loading, impact, repeated handling, snap-fit deformation, protective covers, fixtures, and functional prototypes that require strength together with deformation tolerance. ABS is more appropriate for components that prioritize rigidity, dimensional stability, and surface hardness, such as housings, supports, rigid brackets, and parts requiring local indentation resistance, provided that warping control and printing emissions are properly managed.

In accordance with previous PETG studies [15], [14], [16], PETG demonstrates a more balanced performance between strength and toughness. At high infill, PETG achieves tensile and flexural strength values comparable to ABS while maintaining greater elongation at break and impact strength. This confirms that mechanical performance is not solely determined by density or infill percentage, but also by polymer behavior, cooling conditions, raster bonding, and layer-interface quality. Overall, these findings support performance-based material selection: PETG should be selected when toughness and energy dissipation are dominant requirements, whereas ABS should be selected when hardness and rigidity are more critical.

CONCLUSION

The results of this study confirm that variations in infill percentage play a crucial role in determining the mechanical and physical characteristics of ABS and PETG materials produced through the FDM process. Increasing infill from

25% to 100% consistently increased density and improved tensile strength, flexural strength, impact strength, and hardness. At 100% infill, PETG achieved the highest tensile strength of 40.74 MPa, elongation at break of 16.16%, flexural strength of 59.51 MPa, and impact strength of 0.053 J/mm². ABS showed the highest hardness value, reaching 84.17 Shore D at 100% infill, indicating its stronger surface resistance and rigidity. Thus, PETG provides a better strength-toughness balance for components exposed to dynamic or impact loading, while ABS is more suitable for components requiring high stiffness, dimensional stability, and surface hardness. Future work should include raw replicate data, standard deviation, coefficient of variation, and statistical significance testing to strengthen quantitative comparison between materials and infill levels.

REFERENCES

[1] H. H. Abdulridha, N. H. Obaeed, and A. S. Jaber, "Optimization of fused deposition modeling parameters for polyethylene terephthalate glycol flexural strength and dimensional accuracy," *Adv. Sci. Technol. Res. J.*, vol. 19, no. 4, pp. 50–64, 2025, doi: 10.12913/22998624/200088.

[2] Saeful Rofi Romadhon, Wahyu Hidayat, and Baskara Surya Widagdo, "The Effect of Infill Variation on the Tensile, Bending, Impact, Hardness, and Density Properties of PLA and ABS Materials Produced by FDM," *Multidiscip. Innov. Res. Appl. Eng.*, vol. 2, no. 2, pp. 97–111, Sep. 2025, doi: 10.70935/1nh12096.

[3] R. Ismail *et al.*, "Investigation of the Effect of Nozzle Temperature in Fused Deposition Modelling on the Mechanical Properties and Degradation Behaviour of 3D-Printed PLA/PCL/HA Biocomposite Filaments," *J. Adv. Res. Appl. Mech.*, vol. 135, no. 1, pp. 83–96, Apr. 2025, doi: 10.37934/aram.135.1.8396.

[4] D. Acierno and A. Patti, "Fused Deposition Modelling (FDM) of Thermoplastic-Based Filaments: Process and Rheological Properties—An Overview," *Materials (Basel).*, vol. 16, no. 24, 2023, doi: 10.3390/ma16247664.

[5] R. Ismail *et al.*, "Design, Fabrication, and Performance Testing of PMMA Interference Screws Prepared by 3D Printing Methods," *J. Adv. Res. Appl. Mech.*, vol. 128, no. 1, pp. 86–95, Nov. 2024, doi: 10.37934/aram.128.1.8695.

[6] R. Winarso, P. W. Anggoro, R. Ismail, J. Jamari, and A. P. Bayuseno, "Application of fused deposition modeling (FDM) on bone scaffold manufacturing process: A review," *Heliyon*, vol. 8, no. 11, p. e11701, 2022, doi: 10.1016/j.heliyon.2022.e11701.

[7] M. H. Hosseinzadeh *et al.*, "Beyond standard ABS: Recent advances in modified and composite filaments prepared for fused deposition modeling," *Heliyon*, vol. 11, no. 8, p. e43051, Mar. 2025, doi: 10.1016/j.heliyon.2025.e43051.

[8] R. Gopi Mohan, K. Santhosh, R. V. Iyer, L. K. John, and M. Ramu, "Comparitive analysis of mechanical properties of FDM printed parts based on raster angles," *Mater. Today Proc.*, vol. 47, pp. 4730–4734, 2021, doi: 10.1016/j.matpr.2021.05.649.

[9] S. Guessasma and S. Belhabib, "The Influence of Microstructural Arrangement on the

Failure Characteristics of 3D-Printed Polymers: Exploring Damage Behaviour in Acrylonitrile Butadiene Styrene," *Materials (Basel).*, vol. 17, no. 11, 2024, doi: 10.3390/ma17112699.

[10] P. Rajaee, F. Ashenai Ghasemi, S. A. Sajjadi, and M. Fasihi, "Effect of raster angle on the fracture properties of additively manufactured ABS via essential work of fracture," *J. Appl. Polym. Sci.*, vol. 141, no. 16, 2024, doi: 10.1002/app.55262.

[11] H. Alzyod and P. Ficzere, "Correlation Between Printing Parameters and Residual Stress in Additive Manufacturing: A Numerical Simulation Approach," *Prod. Eng. Arch.*, vol. 29, no. 3, pp. 279–287, 2023, doi: 10.30657/pea.2023.29.32.

[12] C. Yan *et al.*, "PETG: Applications in Modern Medicine," *Eng. Regen.*, vol. 5, no. 1, pp. 45–55, 2024, doi: 10.1016/j.engreg.2023.11.001.

[13] A. Kantaros, M. Katsantoni, T. Ganetsos, and N. Petrescu, "The Evolution of Thermoplastic Raw Materials in High-Speed FFF/FDM 3D Printing Era: Challenges and Opportunities," *Materials (Basel).*, vol. 18, no. 6, p. 1220, Mar. 2025, doi: 10.3390/ma18061220.

[14] S. Guessasma, S. Belhabib, and H. Nouri, "Printability and tensile performance of 3D printed polyethylene terephthalate glycol using fused deposition modelling," *Polymers (Basel).*, vol. 11, no. 7, 2019, doi: 10.3390/polym11071220.

[15] G. Holcomb, E. B. Caldona, X. Cheng, and R. C. Advincula, "On the optimized 3D printing and post-processing of PETG materials," *MRS Commun.*, vol. 12, no. 3, pp. 381–387, 2022, doi: 10.1557/s43579-022-00188-3.

[16] V. E. Alexopoulou, I. T. Christodoulou, and A. P. Markopoulos, "Effect of Printing Speed and Layer Height on Geometrical Accuracy of FDM-Printed Resolution Holes of PETG Artifacts †," *Eng. Proc.*, vol. 24, no. 1, 2022, doi: 10.3390/IECMA2022-12887.

[17] T. Peixoto *et al.*, "Amination of Polymeric Braid Structures to Improve Tendon Healing: An Experimental Comparison," *Macromol. Mater. Eng.*, vol. 308, no. 1, pp. 1–11, 2023, doi: 10.1002/mame.202200426.

[18] M. M. Sultan *et al.*, "Optimization of PETG 3D printing parameters for the design and development of biocompatible bone implants," *Front. Bioeng. Biotechnol.*, vol. 13, no. March, pp. 1–23, 2025, doi: 10.3389/fbioe.2025.1549191.

[19] Y. Y. Aw, C. K. Yeoh, M. A. Idris, P. L. Teh, K. A. Hamzah, and S. A. Sazali, "Effect of printing parameters on tensile, dynamic mechanical, and thermoelectric properties of FDM 3D printed CABS/ZnO composites," *Materials (Basel).*, vol. 11, no. 4, 2018, doi: 10.3390/ma11040466.

[20] D. Mahandika and H. Sukma, "Analisa Hasil Cetak 3D Printer Terhadap Pengujian Tarik Material ABS+ dengan Variasi Densitas Infill," *Teknobiz J. Ilm. Progr. Stud. Magister Tek. Mesin*, vol. 15, no. 1, pp. 50–54, 2025, doi: 10.35814/teknobiz.v15i1.8556.

[21] R. Srinivasan, W. Ruban, A. Deepanraj, R. Bhuvanesh, and T. Bhuvanesh, "Effect on infill density on mechanical properties of PETG part fabricated by fused deposition modelling," *Mater. Today Proc.*, vol. 27, pp. 1838–1842, 2020, doi: https://doi.org/10.1016/j.matpr.2020.03.797.

[22] E. Hozdić and E. Hozdić, "Influence of Infill Structure Shape and Density on the Mechanical Properties of FDM 3D-Printed PETG and PETG+CF Materials," *Adv.*

Technol. Mater., vol. 49, no. 2, pp. 15–27, 2024, doi: 10.24867/atm-2024-2-002.

[23] R. Kumaresan and K. Kanny, "Advanced RSM-driven optimisation for enhancing the mechanical performance of FDM-printed PETG: A correlated microstructural and mechanical property investigation," Polymers, vol. 17, no. 23, p. 3175, 2025, doi: 10.3390/polym17233175.

[24] K. N. Gunasekaran, V. Aravinth, C. B. M. Kumaran, K. Madhankumar, and S. P. Kumar, "Investigation of mechanical properties of PLA printed materials under varying infill density," *Mater. Today Proc.*, vol. 45, pp. 1849–1856, 2021, doi: 10.1016/j.matpr.2020.09.041.

[25] E. A. Syaefudin, A. Kholil, M. Hakim, D. A. Wulandari, Riyadi, and E. Murtinugraha, "The effect of orientation on tensile strength 3D printing with ABS and PLA materials," *J. Phys. Conf. Ser.*, vol. 2596, no. 1, 2023, doi: 10.1088/1742-6596/2596/1/012002.